Controlling the Morphology of CVD Films

Hendrik J. Viljoen
Dept. of Chemical Engineering, University of Nebraska at Lincoln, Lincoln, NE 68588

Jacob J. Thiart and Vladimir Hlavacek
Lab. for Ceramic and Reaction Engineering, Dept. of Chemical Engineering,
State University of New York at Buffalo, Amherst, NY 14260

The morphology of the gas-solid interface during typical chemical vapor deposition (CVD) processes is investigated. The dynamic behavior of the interface depends on many factors, including local curvature of the film, reactant diffusion, adsorption equilibrium, surface kinetics, and mobility of adatoms. These factors depend on material properties of the system and reactor conditions, such as the deposition temperature and pressure. A 2-D model proposed describes the evolution of the interface in Cartesian coordinates under the influence of stabilizing and destabilizing effects. A linear stability analysis is used to predict under which conditions a planar interface becomes unstable. Stability criteria of a simplified 1-D analysis is not necessarily valid if the real system has more than one dimension. The substrate temperature and reactor pressure are important factors affecting the stability of film growth and thus the morphology of CVD films. An increase in temperature stabilizes planar film growth if the deposition is diffusion-limited, but destabilizes it if the process is reaction-controlled. The reactor pressure has a destabilizing effect on planar film growth during a typical CVD process.

Introduction

The phenomenal progress in the computer industry is proof of the industrial success of producing more advanced microelectronics devices. The quest for even higher performance requires the development of new processing techniques and better control of existing ones. Microelectronic devices are almost exclusively produced by vapor deposition techniques, including processes utilizing physical vapor deposition (PVD) and those using chemical vapor deposition (CVD). Examples of PVD technology include evaporation processes, such as activated reactive evaporation (ARE), molecular beam epitaxy (MBE), ion plating, and sputter deposition processes (Vossen and Kern, 1978, 1991; Bunshah, 1982; Habig, 1986).

Chemical vapor deposition (CVD), also called *thermal* CVD, makes use of a chemical reaction in the gas phase close to or on the surface of the film to deposit the desired material. Variations of the basic technique include plasma-enhanced CVD (PECVD), low-pressure CVD (LPCVD), metal-organic vapor-phase epitaxy (OMVPE), and photo-CVD (Vossen and Kern, 1978, 1991). Nowadays, the majority of industrially important thin films are produced by CVD and the demands on the properties of the films have become increasingly difficult to achieve. A CVD process has to produce thin films with reproducible and controllable properties, which include its purity, composition, thickness, microstructure, and its surface morphology. The thermal and electrical properties of the film are very important and it has been found that thin film performance is adversely affected by factors like porosity, inhomogeneities and inclusions, and zones with different morphology. The control of film quality is strongly coupled to the control of conditions in the deposition chamber. For CVD processes, the substrate temperature, gas feed composition, chamber pressure, and gas flow rates are all crucial variables which can be controlled externally.

One of the characteristics of vapor deposition processes is a slow rate of deposition, especially for PVD processes. It is typically between 1 and 10 μm/h, but for CVD it can be much higher. Ideally, one would like the highest deposition rate possible, but it has been found that the uniformity of the film decreases with increasing deposition rate. A balance has to be found between the quality of the film and the processing time, reactor throughput, and related economic considerations.

Correspondence concerning this article should be addressed to H. J. Viljoen.

The characterization of film morphology and the control of it have become increasingly important as the need for higher performance of thin film applications continue. The details of the surface morphology seem to be a complex and sensitive function of both substrate and film materials, as well as the conditions under which the film is deposited.

Several researchers have reported morphological phenomena which were observed experimentally in vapor deposition processes. The phenomena observed in CVD are sometimes contradictory to what have been found in PVD processes. The change in morphology with temperature is one example. In PVD processes such as sputtering and ARE it has been observed that the temperature has a strong effect on the film morphology (Movchan and Demchishin, 1969; Thornton, 1974; Mazor et al., 1988). A structure zone model or SZM (Messier and Yehoda, 1985; Messier, 1986) was used to classify the surface morphology. Three zones of different morphology were identified, which could be attributed to three different temperature ranges. The ranges are defined by the ratio of the substrate temperature (T) and the melting point of the coating material (T_m). The morphology in zone 1 ($T/T_m < 0.25$-0.3) consisted of tapered crystallites with domed tops which increase in width with temperature. In zone 2 (defined as $0.25\text{-}0.3 < T/T_m < 0.45$) columnar grains with a smooth surface were observed and in zone 3 (where $T/T_m > 0.45$) equiaxed grains with a bright surface. Therefore, an increase in temperature results in a smoother surface. Chin et al. (1977) studied the effect of reactor conditions on the morphology of *SiC* films deposited with CVD and observed that strongly faceted structures were deposited at higher deposition temperatures and lower pressures. Smooth deposits with circular caps were obtained at lower temperatures and higher pressures. They also identified three zones with different morphology, depending on the temperature. At low temperature, in zone 1 the deposition was smooth and featureless, zone 2 consisted of the domed structures, and zone 3 of the faceted structures. Note that these zones differ from those identified for PVD processes. Schmidt (1991) also observed with the CVD of CrB_2 on a tungsten wire that the surface morphology changed from smooth to nodular and then to dendritic, with increasing temperature. Hartmann et al. (1991) studied the CVD of *ZnSe* from *Zn-Se-*H_2*-Ar* and *Zn-*H_2*Se-Ar*, and found the film structure to change from fine-grained to coarse to dendritic with increasing temperature.

Contradictory phenomena were also observed for the rate of deposition as a function of temperature. Raghuram and Bunshah (1972) studied the effect of temperature on the deposition rate of *TiC* by activated reactive evaporation and found that the deposition rate decreased with increasing temperature. Parretta et al. (1991) studied the formation of *SiC* by CVD from $SiCl_4$, C_3H_8, and H_2 and found that the deposition rate increased with temperature. This trend was also observed by Chin et al. (1977).

The different trends are due to the inherently different characteristics of PVD and CVD processes. PVD is carried out under high vacuum, with the pressure typically in the range of 10^{-8} to 10^{-3} torr. Under these conditions the mean free path (MFP) is very large compared to the distance between the source and the substrate, and the characteristic length of morphological features. The Knudsen number (Friedlander, 1977) is very large ($Kn \gg 1$) and the deposition is essentially ballistic. The reactor pressure during CVD is typically much higher, 10^{-3} *torr* to *atmospheric* (Habig, 1986), and the transport of species to the surface can be either ballistic or diffusion-driven, depending on the value of Kn. The characteristics of surface processes also differ between PVD and CVD. The rate of reevaporation can increase with temperature during a PVD process, which has an adverse effect on the deposition rate, whereas the rate of chemical reaction (leading to a solid deposit) on the surface can increase during CVD, thus resulting in a higher deposition rate. The adatom mobility on the surface is another important factor which greatly affects the morphology of the film and it has been the primary correlation factor in the so-called structure zone models (SZM).

Several studies have been undertaken to explain the experimentally observed phenomena. These have taken the form of computer simulations and Monte Carlo studies of the ballistic deposition of discrete particles (Henderson et al., 1974; Srolovitz, 1986; Cooke and Harris, 1989; Tait et al., 1990), or continuum models (Blech, 1970; Lichter and Chen, 1986; Bernoff and Lichter, 1989; Bales and Zangwill, 1991). Dirks and Leamy (1977) studied the problem on discrete particle level and suggested that the columnar microstructure found in vapor-deposited films was due to self-shadowing of the vapor beam by the growing film. This occurs during low adatom mobility. Srolovitz and his coworkers (Mazor et al., 1988, 1989; Srolovitz et al., 1988) presented a continuum model for the growth of columnar microstructures in thin films. They considered a constant deposition flux to the surface and included the effects of surface diffusion and curvature on the morphology. Their model described one-dimensional growth and was used to predict the columnar form of films observed in zone 2 during PVD processes. Srolovitz (1986) did a Monte Carlo study which illustrated how the characteristic grain size increased with time during deposition. This effect has been demonstrated very often and several studies have shown that morphological features of thin films typically grow in time in the form of a cone. There is a competition for growth which results in some cones *dying off* and others growing in size (Messier, 1986). The average grain size thus increases with time.

An important difference between modeling CVD and PVD lies in the transport mechanism to the surface. Under high pressure CVD (0.1 to 1 atm) the MFP is much shorter than the typical length of morphological features and the value of the Knudsen number is therefore very small. Accordingly, transport of the reactants to the surface is diffusion-driven (not ballistic) and a continuum model is appropriate.

Van den Brekel and Jansen (1978a, 1978b) studied the stability of a flat interface during CVD processes. Their model included a stagnant boundary layer, and the surface reaction was assumed to be proportional to the supersaturation. They considered a reversible chemical reaction and used the Gibbs-Thompson relation to relate the equilibrium concentration on the surface to the curvature of the film. In their model capillarity is the only stabilizing factor, and the important effect of surface diffusion was neglected. They found that vapor growth is essentially an unstable process. The study was extended to nonisothermal conditions, and they found that their results remained qualitatively the same. Their study suggested that the effect of nonisothermal conditions was most dominant if the process is diffusion-limited. Bales et al. (1989) did a numerical treatment of the Van den Brekel-Jansen model and considered cases where the process was either diffusion-limited

or reaction-limited. Under diffusion-limited growth, they found the morphology to be fingerlike and very similar to what have been found for the Hele-Shaw problem (Pelce, 1988). In cases where growth was reaction-controlled, the morphology was similar to the results predicted by Kardar et al. (1986) and consisted of circular arcs, which exhibited the same *growth-death* phenomenon as observed experimentally in many vapor deposition processes.

Palmer and Gordon (1988, 1989) also neglected the effect of a temperature gradient in the growing film. They included the effects of surface diffusion, gas diffusion, and reevaporation. It was assumed that the reaction took place in the gas phase; only adsorption and reevaporation took place on the surface. They considered a stagnant boundary layer which became thinner as time progressed and the film grew. Gas diffusion was identified as the destabilizing factor, while surface diffusion and reevaporation are the stabilizing factors. Ananth and Gill (1992) included the effect of heat transfer in the solid film but neglected the effect of radiation and the temperature dependence of material properties. They found that heating from below the substrate tends to stabilize the film in a cold wall reactor. They also found that capillarity may have a significant effect as a stabilizing factor.

Many studies have also been done on the stability of the solidification of crystals from a melt (Mullins and Sekerka, 1964; Koo et al., 1992). This problem (liquid-solid phase) is analogous to vapor deposition and the growth of a solid film into the gas phase. The solidification process can be controlled by the liquid-phase temperature gradient, thus diffusion of heat, which is similar to solid film growth in a diffusion-limited CVD process. In this case there is a diffusion of reactants to the growing interface. More examples of analogies between different systems where the dynamics of curved interfaces have been studied can be found in Pelce (1988).

The aim of this article is to develop a continuum model which realistically describes the evolution of a solid film during typical CVD processes. In the light of the increasingly stringent demands that are placed on thin film properties, it is important that a realistic model should not only be able to describe and confirm observed phenomena, but it should also lend itself to numerical solution from which it will be able to predict morphology for specific conditions. It will then be possible to identify the optimal reactor conditions which will ensure uniform film growth and thus effective control over desired film properties.

We will consider a planar interface as the basic solution and study its linear stability under the influence of stabilizing and destabilizing effects. These include surface diffusion, gas diffusion, capillarity, the surface reaction, and the curvature of the film. Furthermore, we will study the effect of reactor conditions such as the substrate temperature and chamber pressure on the stability of the basic solution and also illustrate the difference between results obtained with a two-dimensional and a one-dimensional analysis.

Model of Film Evolution

Consider the growth of an amorphous solid film during a typical high pressure (0.1 to 1 atm) CVD process. At this pressure the mean free path (MFP) in the gas is very short compared to the typical length of surface features and one cannot consider the deposition to be ballistic. More appropriately, we consider the transport of reactant through a boundary layer by diffusion and assume that the concentration of the reactant is constant in the bulk fluid. The processes taking place on the film surface are adsorption/desorption (chemisorption) of the reactant, chemical reaction on the surface to form the solid product, and surface diffusion of the product molecules in the plane of the surface. Let us assume the adsorption of reactants is governed by an adsorption/desorption equilibrium, but the surface reaction is taken as irreversible and the reaction order is *one*.

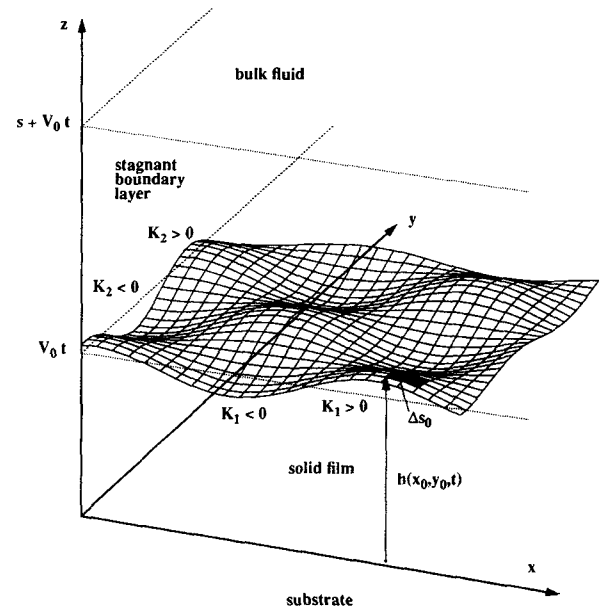

Figure 1. Growing film.

A Cartesian coordinate system is used, which is appropriate for deposition on planar substrate surfaces. However, it can also be used for cylindrical substrates where the film thickness is much smaller than the substrate diameter. The Cartesian coordinate system becomes less appropriate when CVD on a fiber or metal wire is considered.

The principle of conservation of mass is used to derive an equation for the evolution of the solid film. The flux of reactant to the surface results in film growth and any surface protrusions are smoothed by surface diffusion. This effect depends strongly on the mobility of the adatoms, which depends on the temperature. One can define an effective diffusivity, D_e, which is related to the surface diffusivity, D_s, as follows (Mazor et al., 1988):

$$D_e = \frac{D_s \sigma_s \Omega^2 \alpha}{K_B T} \tag{1}$$

where Ω is the molecule's volume, α is the number of molecules per unit surface area, σ_s is the surface energy density, and $K_B T$ is the thermal energy. The surface diffusivity, D_s, has a typical Arrhenius temperature dependence.

Figure 1 shows a representation of the growing film. The substrate is located at $z=0$ and the film thickness at any position (x, y) along the substrate and any point in time t is given by $h(x, y, t)$. Since the model gives the height of the film as a function of x and y, the development of vertical profiles (where $h_x \to \infty$ or $h_y \to \infty$) is not permitted. The range

of the horizontal coordinates x and y is taken as infinite, since the scale for morphological features is typically much smaller than the dimensions of the substrate, hence periodic boundary conditions are in order. This assumption must be revised for small-area substrates, such as those found in many microelectronic applications.

The equation for the change in height $h(x, y, t)$ of the surface is given by (see Appendix I for the derivation):

$$h_t = h_x J_1 + h_y J_2 + J_3 + D_e\left[\left(\frac{\mathcal{K}_{1x}}{\sqrt{1+h_x^2+h_y^2}}\right)_x + \left(\frac{\mathcal{K}_{2y}}{\sqrt{1+h_x^2+h_y^2}}\right)_y\right] \quad (2)$$

where J_1, J_2, and J_3 are the flux components in the x, y, and z directions respectively, and $\mathcal{K}_1$ and $\mathcal{K}_2$ are the x and y components of the local curvature, defined as:

$$\mathcal{K}_1 = -\frac{h_{xx}}{(1+h_x^2+h_y^2)^{3/2}}, \quad \mathcal{K}_2 = -\frac{h_{yy}}{(1+h_x^2+h_y^2)^{3/2}}. \quad (3)$$

The subscripts t, x, and y denote partial differentiation with respect to these variables.

The first terms on the righthand side of Eq. 2 represent the growth of the film as a result of the flux of reactant to the interface, and the last term represents the effect of surface diffusion. Diffusional resistance in the boundary layer will result in higher reactant concentration and thus enhanced deposition on convex parts of the surface relative to concave parts (viewed from the gas phase). This is a destabilizing effect, whereas surface diffusion tends to smooth irregularities and is therefore a stabilizing effect on planar film growth. The relative magnitude of these effects will determine whether the growing interface is inherently stable, or not.

The temperature field in the solid film and gas boundary layer depends strongly on the configuration of the reactor. In a cold wall reactor the substrate is heated (resistively) and maintained at a higher temperature than the outer walls. Ananth and Gill (1992) studied heat transfer in a cold wall reactor and showed that the temperature gradient in the solid film has a stabilizing effect on planar film growth. However, their study neglected the temperature dependence of material properties and the contribution of radiation, which is the main mode of heat transfer at such elevated temperatures. We will consider deposition in a hot wall reactor, where external heating of the substrate is achieved through radiation. Temperature gradients are typically less severe and in the opposite direction than those in the cold wall configuration.

To determine the temperature field in the reactor, one has to write energy balance equations for the gas phase, solid film, and the substrate. These equations will be coupled to the concentration balance in the gas phase and the equation for surface evolution. The formulation of the problem is further complicated by the temperature dependence of material properties, such as the gas diffusivity (D_f), surface diffusivity (D_e), and capillary length (Γ), and temperature dependence of system parameters, such as the reaction rate constant (k) and the adsorption equilibrium constant (K_{AD}). However, the problem can be made more tractable by assuming that the temperature of the solid surface is kept constant at the desired deposition temperature. This is not unrealistic, since a large temperature gradient of 500 K/cm as reported by Ananth and Gill (1992) translates to only 0.5 K difference through a 10 μm film. The reactants are usually present in very dilute concentrations in the bulk fluid, and we assume that the heat effect of the surface reaction does not have a significant influence on the temperature of the substrate, film, or gas above it (Roenigk and Jensen, 1985). Under these circumstances, it can be assumed that the substrate, film, and gas immediately above it are in thermal equilibrium and temperature becomes a constant parameter.

Concentration balance

With the assumption of constant film temperature, the concentration profile in the stagnant boundary layer still has to be determined. We assume the boundary layer thickness, s, remains constant. For most cases the value of s is much greater than the characteristic length of any disturbances on the surface, which means that the boundary layer can be considered as semi-infinite. However, we will keep the analysis general and assume a finite boundary layer thickness.

The concentration balance in the boundary layer becomes:

$$\frac{\partial C}{\partial t} = D_f(\nabla^2 C) \quad (4)$$

where

$$\nabla^2(\cdot) \equiv \frac{\partial^2(\cdot)}{\partial x^2} + \frac{\partial^2(\cdot)}{\partial y^2} + \frac{\partial^2(\cdot)}{\partial z^2}.$$

In the laboratory framework the interface is moving as a result of solid film growth, and you would therefore expect a convection term in the governing equations, but note that this is not the case. The boundary layer is stagnant with respect to the moving interface and its thickness remains constant. Diffusion of reactant is the only mode of transport. If the film grows at a constant rate V_0, the boundary conditions in the z-direction are:

$$C = C_b \quad \text{at} \quad z = s + V_0 t \quad (5)$$

$$D_f(\nabla C \cdot \boldsymbol{n}) = R(C) \quad \text{at} \quad z = h(x, y, t) \quad (6)$$

where $R(C)$ is the reaction or consumption term and has to include the contributions of adsorption, desorption, and the chemical reaction. The range in the x and y directions is assumed as infinite and the lateral boundary conditions are taken as periodic.

The surface reaction is assumed to be irreversible and first-order with respect to the concentration of species on the surface. The effect of curvature and capillarity on the adsorption equilibrium is governed by the Gibbs-Thompson relation (Van den Brekel and Jansen, 1978). This equation relates the adsorbed concentration to the gas concentration above it:

$$C_s = K_{AD}(1 - \Gamma\mathcal{K}_1)(1 - \Gamma\mathcal{K}_2)C \quad (7)$$

where K_{AD} is an adsorption/desorption equilibrium constant and Γ is the capillary length, defined as:

$$\Gamma = \frac{\Upsilon\gamma}{R_0 T_s}.$$

The capillarity is an effect which exists as a result of the surface energy at a curved surface and it inhibits the adsorption of reactants on convex parts of the film relative to concave parts. Assuming the rate of consumption of the reactant is first-order with respect to the concentration on the surface, C_s, the reaction term is given by:

$$R(C) = kK_{AD}(1-\Gamma\mathcal{K}_1)(1-\Gamma\mathcal{K}_2)C \tag{8}$$

where k is the chemical reaction rate constant which has an Arrhenius dependence on temperature. Combining Eqs. 6 and 8, the boundary condition at the surface is given by:

$$D_f(\nabla C\cdot\boldsymbol{n}) = kK_{AD}(1-\Gamma\mathcal{K}_1)(1-\Gamma\mathcal{K}_2)C \quad \text{at} \quad z = h(x, y, t). \tag{9}$$

The reaction term depends on the local curvature of the film and this couples the concentration balance to the equation of film evolution.

Coordinate transformation

To write the moving boundary value problem in a more convenient form, we introduce a transformation which allows the origin of the vertical coordinate to move with the growing film. Thus,

$$z^* = z - V_0 t \tag{10}$$

where V_0 is a reference growth rate, which we take as the constant growth rate under planar film growth. The transformation is applied to the concentration balance equations and the equation for surface evolution. The transformation essentially affects only the derivative with respect to time and not the spatial derivatives. Equation 4 becomes:

$$\frac{\partial C}{\partial t} = D_f(\nabla^{*2}C) + V_0\frac{\partial C}{\partial z^*}, \tag{11}$$

where

$$\nabla^{*2}(\cdot) \equiv \frac{\partial^2(\cdot)}{\partial x^2} + \frac{\partial^2(\cdot)}{\partial y^2} + \frac{\partial^2(\cdot)}{\partial z^{*2}}.$$

Note that the transformation has introduced a convection term into the concentration balance. The boundary conditions become:

$$C = C_b \quad \text{at} \quad z^* = s \tag{12}$$

$$D_f(\nabla C\cdot\boldsymbol{n}) = kK_{AD}(1-\Gamma\mathcal{K}_1) \times (1-\Gamma\mathcal{K}_2)C \quad \text{at} \quad z^* = h^*(x, y, t). \tag{13}$$

The term $\nabla C\cdot\boldsymbol{n}$ describes the diffusive flux of reactant to the surface, and is given by:

$$\nabla C\cdot\boldsymbol{n} = -\frac{h_x^*}{\sqrt{1+h_x^{*2}+h_y^{*2}}}\frac{\partial C}{\partial x} - \frac{h_y^*}{\sqrt{1+h_x^{*2}+h_y^{*2}}}\frac{\partial C}{\partial y} + \frac{1}{\sqrt{1+h_x^{*2}+h_y^{*2}}}\frac{\partial C}{\partial z^*}. \tag{14}$$

The position of the interface is $z = h$ and thus in the transformed coordinate system $z^* = h^*$. Therefore, h_t is equivalent to $(h_t^* + V_0)$. The equation describing the evolution of the film becomes:

$$h_t^* + V_0 = h_x^* J_1 + h_y^* J_2 + J_3 + D_e\left(\left[\frac{\mathcal{K}_{1x}}{\sqrt{1+(h_x^*)^2+(h_y^*)^2}}\right]_x + \left[\frac{\mathcal{K}_{2y}}{\sqrt{1+(h_x^*)^2+(h_y^*)^2}}\right]_y\right). \tag{15}$$

Dimensionless equations

Define a characteristic length, L, as scale:

$$L = \sqrt{\frac{D_e}{\delta V_0}}. \tag{16}$$

The following dimensionless variables are used:

$$\xi = \frac{x}{L}, \quad \eta = \frac{y}{L}, \quad \zeta = \frac{z^*}{L}, \quad \mathcal{C} = \frac{C}{C_b}, \quad H = \frac{h^*}{L}, \quad \tau = \frac{tV_0}{L}, \quad \kappa_1 = L\mathcal{K}_1, \quad \kappa_2 = L\mathcal{K}_2.$$

The concentration balance equation becomes:

$$\frac{\partial \mathcal{C}}{\partial \tau} = \frac{1}{Pe}(\nabla^2\mathcal{C}) + \frac{\partial \mathcal{C}}{\partial \zeta} \tag{17}$$

where ∇^2 now represents

$$\nabla^2(\cdot) \equiv \frac{\partial^2(\cdot)}{\partial \xi^2} + \frac{\partial^2(\cdot)}{\partial \eta^2} + \frac{\partial^2(\cdot)}{\partial \zeta^2}.$$

The boundary conditions are

$$\mathcal{C} = 1 \quad \text{at} \quad \zeta = \frac{s}{L}, \tag{18}$$

$$\frac{1}{Pe}(\nabla\mathcal{C}\cdot\boldsymbol{n}) = \frac{kK_{AD}}{V_0}\left(1-\frac{\Gamma}{L}\kappa_1\right)\left(1-\frac{\Gamma}{L}\kappa_2\right)\mathcal{C} \quad \text{at} \quad \zeta = H \tag{19}$$

where

$$Pe = \frac{V_0 L}{D_f}.$$

The Peclet number, Pe, gives us an indication of the relative magnitude of convection and diffusion effects. In this problem one would expect the value of Pe to be extremely small since film growth occurs at a slow rate. Later we will see that this is indeed the case. Note that the boundary conditions in the horizontal directions are taken as periodic.

The equation for surface evolution becomes:

$$\frac{\partial H}{\partial \tau}+1=\frac{\rho}{Pe}\left[-H_\xi\frac{\partial \mathcal{C}}{\partial \xi}-H_\eta\frac{\partial \mathcal{C}}{\partial \eta}+\frac{\partial \mathcal{C}}{\partial \zeta}\right]+\chi\left(\left[\frac{\kappa_{1\xi}}{\sqrt{1+H_\xi^2+H_\eta^2}}\right]_\xi+\left[\frac{\kappa_{2\eta}}{\sqrt{1+H_\xi^2+H_\eta^2}}\right]_\eta\right). \quad (20)$$

where ρ and χ are dimensionless parameters. Note that κ_1 and κ_2 now represent the dimensionless components of the curvature.

The governing equations for the concentration balance in the gas boundary layer and the growth of the solid film represent a system of coupled nonlinear partial differential equations (PDEs). These cannot generally be solved analytically. If one invokes some simplifying assumptions, it is possible to decouple the concentration balance and the equation for film growth, and an approximate solution may be found. For example, if one assumes the flux of reactant to the interface is constant and independent of the surface morphology, the system of equations simplify to an initial value problem (in H), which can easily be solved numerically (see Mazor et al., 1988, 1989, for the solution of a related problem in PVD).

In a future contribution we will focus on the approximate solution of our system of equations under specific conditions, as well as under more general conditions where the complete problem is solved numerically. Valuable information about the process can, however, be obtained without having to solve the governing equations, if a linear stability analysis is performed. In the next section, we study the stability of a flat interface subjected to a small periodic perturbation.

Basic Solution

The most desirable mode of growth for ensuring a uniform film is the planar surface. Thus, for the basic solution, the height of the film does not depend on ξ or η, and the film grows at a constant rate in a planar form. Under these conditions, the concentration in the boundary layer also depends on ζ only and the curvature, κ_1, $\kappa_2 \equiv 0$. The concentration balance and corresponding boundary conditions become:

$$\frac{1}{Pe}\left[\frac{\partial^2 \mathcal{C}_0}{\partial \zeta^2}\right]+\frac{\partial \mathcal{C}_0}{\partial \zeta}=0, \quad (21)$$

$$\mathcal{C}_0=1 \quad \text{at} \quad \zeta=\frac{s}{L} \quad (22)$$

$$\frac{1}{Pe}\frac{\partial \mathcal{C}_0}{\partial \zeta}=\frac{kK_{AD}}{V_0}\mathcal{C}_0 \quad \text{at} \quad \zeta=H=0 \quad (23)$$

with periodic boundary conditions in ξ and η.

The solution is given by:

$$\mathcal{C}_0(\zeta)=a+b\exp[-Pe\zeta] \quad (24)$$

where a and b are constants which depend on the reactor conditions:

$$a=\frac{(V_0+kK_{AD})/kK_{AD}}{(V_0+kK_{AD})/kK_{AD}-\exp[-Pes/L]},$$

$$b=\frac{-1}{(V_0+kK_{AD})/kK_{AD}-\exp[-Pes/L]}.$$

The value of the growth rate V_0 is determined by substituting the basic concentration profile in the simplified form of Eq. 20. This yields the expression:

$$\exp[-Pes/L]-(V_0+kK_{AD})/kK_{AD}+\rho=0 \quad (25)$$

which is a nonlinear function of V_0 (since Pe also depends on V_0) and has to be solved for specific reactor conditions.

Linear Stability Analysis

The two most critical factors which determine film surface stability are the rate of deposition, which depends on the surface reaction and thus the flux to the surface, and the surface mobility of product particles. If the destabilizing force of the rate of deposition is larger than the stabilizing force of surface mobility, the growing interface is inherently unstable. When the deposition rate is low and the surface mobility of adsorbed species is high, the film will be of high quality, near theoretical density and the growing interface will be planar. We consider planar film growth as a necessary condition for producing uniform films.

To determine under which conditions the planar form of growth becomes unstable, a linear stability analysis is performed. We will consider the perfectly flat surface and perturb this basic condition to study the stability of the planar film. The perturbed concentration and height of the film is given by:

$$\mathcal{C}(\xi,\eta,\zeta,\tau)=\mathcal{C}_0(\zeta)+\epsilon\mathcal{C}_1(\xi,\eta,\zeta,\tau)+\ldots \quad (26)$$

$$H(\xi,\eta,\tau)=H_0+\epsilon H_1(\xi,\eta,\tau)+\ldots \quad (27)$$

where ϵ is a small perturbation parameter and $\mathcal{C}_0(\zeta)$ is given by Eq. 24. In this analysis we will consider only terms of $O(1)$ and $O(\epsilon)$. Note that in the moving coordinate system $H_0=0$. Consider trial functions of the form:

$$\mathcal{C}_1(\xi,\eta,\zeta,\tau)=C^*(\zeta)e^{i\mu_1\xi+i\mu_2\eta+\omega\tau} \quad (28)$$

$$H_1(\xi,\eta,\tau)=H^*e^{i\mu_1\xi+i\mu_2\eta+\omega\tau} \quad (29)$$

Upon substitution of the trial functions in Eq. 17, one obtains [to $O(\epsilon)$]

$$\omega C^*=\frac{1}{Pe}[C^*_{\zeta\zeta}-\mu_1^2C^*-\mu_2^2C^*]+C^*_\zeta \quad (30)$$

which suggests a solution of the form:

$$C^*(\zeta)=Ae^{\psi_1\zeta}+Be^{\psi_2\zeta} \quad (31)$$

where A and B are constants and ψ_1 and ψ_2 are the solutions of the characteristic equation.
Thus,

$$\psi_{1,2}=\frac{-Pe\pm\sqrt{Pe^2+4(\omega Pe+\mu_1^2+\mu_2^2)}}{2} \quad (32)$$

where we take $\psi_2<\psi_1$. By substituting the trial functions in

the growth equation (Eq. 20), we obtain the following eigenvalue problem [$O(\epsilon)$]:

$$\omega H^* = \frac{\rho}{Pe}[\psi_1 A + \psi_2 B + Pe^2 b H^*] - \chi(\mu_1^4 + \mu_2^4)H^*. \quad (33)$$

Note that although we have retained the ξ and η components of the diffusive flux to the surface in our growth Eq. 20, they appear to be terms of $O(\epsilon^2)$ and therefore do not enter the eigenvalue problem in the linear stability analysis. Also note that b is a negative constant.

By applying boundary condition 18, one can write the constant A in terms of B and substitute this relation in Eq. 33 and in the other boundary condition, Eq. 19. Thus, we obtain the following two equations:

$$[\omega - \rho Pe\, b + \chi(\mu_1^4 + \mu_2^4)]H^* + \left[\frac{\rho}{Pe}(\psi_1\beta - \psi_2)\right]B = 0$$

$$\left[Pe\, b\left(1 + \frac{kK_{AD}}{V_0}\right) + \frac{kK_{AD}\Gamma}{V_0 L}(a+b)(\mu_1^2 + \mu_2^2)\right]H^* + \left[\left(\frac{\psi_2 - \psi_1\beta}{Pe}\right) - \frac{kK_{AD}}{V_0}(1-\beta)\right]B = 0$$

where $\beta = \exp[(\psi_2 - \psi_1)s/L]$ and the other parameters are defined in the notation section. The dispersion relation is obtained from these equations:

$$\omega = b\rho Pe - \chi(\mu_1^4 + \mu_2^4) - \frac{(\psi_2 - \psi_1\beta)\rho}{\psi_2 - \psi_1\beta - \frac{PekK_{AD}}{V_0}(1-\beta)} \times \left[Pe\, b\left(1 + \frac{kK_{AD}}{V_0}\right) + \frac{kK_{AD}(a+b)\Gamma}{V_0 L}(\mu_1^2 + \mu_2^2)\right]. \quad (34)$$

The eigenvalue, ω, enters the dispersion relation in the terms containing ψ_1, ψ_2, and β, and the equation is therefore a highly nonlinear function of ω. The dispersion relation is used to determine whether the planar film will become unstable for specific reactor conditions, or not. For specific conditions and for a specific choice of the wave numbers μ_1 and μ_2, one can determine the value of ω from Eq. 34. The eigenvalue(s) can be complex, thus $\omega = \omega_R + i\omega_I$. In this case, if the real part of the leading eigenvalue becomes zero while ω_I is nonzero, the solution for slightly unstable conditions is in the form of a traveling wave with a period of $2\pi/\omega_I$. The spectrum of Eq. 34 has real and complex elements, but the leading eigenvalue was found to be real for all cases investigated. Therefore, we consider conditions which lead to a principle exchange of stability, that is, where the leading eigenvalue is real and changes sign from negative to positive.

The growth of the planar surface is stable or unstable depending on the value of ω. If $\omega > 0$ for specific reactor conditions, any perturbation of the surface will grow unstably and if $\omega < 0$, perturbations will disappear and the planar surface will be the stable mode of propagation. The dispersion relation is essentially an equation in which ω is a nonlinear function of the wave numbers μ_1 and μ_2. These wave numbers are related to the wavelength of the perturbation in the ξ and η directions by:

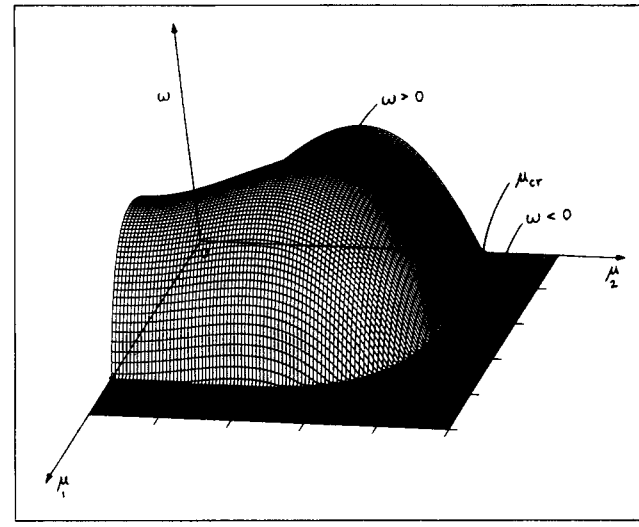

Figure 2. Dispersion relation as a function of the wave numbers, μ_1 and μ_2.

$$\lambda_1 = 2\pi/\mu_1, \quad \lambda_2 = 2\pi/\mu_2.$$

Figure 2 presents the eigenvalue, ω, as a function of the wave numbers μ_1 and μ_2 for a set of realistic parameters as indicated in Table 1. Note that the results are symmetrical around μ_1 and μ_2, since we assume isotropic conditions, where phenomena are identical in the ξ and η directions. The graph is clipped at $\omega = 0$ to show the line representing critical conditions, that is, where a perturbation will neither grow or decay with time. The values of the critical wave numbers can be obtained by setting $\omega = 0$ in Eq. 34 and solving the resulting equation for either $\mu_{1_{cr}}$ or $\mu_{2_{cr}}$. The critical wavelengths, $\lambda_{1_{cr}}$ and $\lambda_{2_{cr}}$, are then obtained from the relation $\lambda_{cr} = 2\pi/\mu_{cr}$.

By determining the critical wavelengths at different substrate temperatures, pressures, and so on, the dispersion relation enables us to study the effect of reactor conditions on the stability of the planar film.

Simplified Dispersion Relation

The dispersion relation can be simplified significantly if one compares the order of magnitude of different terms. In typical CVD processes, the growth rate is very slow and the Peclet number is much smaller than unity. In fact, a typical value for

Table 1. Set of Parameter Values for Plot of Dispersion Relation in Figure 2

Parameter	Value
T (K)	1,600
s (m)	1.0×10^{-3}
δ (m)	1.0×10^{-10}
ρ	1.0×10^{-5}
kK_{AD} (m/s)	10.0
D_f (m^2/s)	3.47×10^{-7}
D_e (m^4/s)	2.61×10^{-28}
Γ (m)	5.0×10^{-12}
V_0 (m/s)	3.47×10^{-9}
L (m)	2.74×10^{-5}
Pe	2.74×10^{-7}
χ	3.65×10^{-6}

Pe under these conditions is 10^{-7} to 10^{-12}. Therefore, the effect of convection plays almost no role in such a process. A typical value of the characteristic length $L \approx 10^{-5}$ to 10^{-7} m, while the value of s is in the order of 10^{-3} m, so that $\exp[-Pes/L] \approx 1 - Pes/L$. With this approximation $V_0 \approx \rho k K_{AD}/(1 + s k K_{AD}/D_f)$. Also, $b \approx -kK_{AD}/[(V_0(1 + s k K_{AD}/D_f)]$ and $a + b \approx 1/(1 + s k K_{AD}/D_f)$. Under these circumstances:

$$\omega = -Pe - \chi(\mu_1^4 + \mu_2^4) + \frac{(\psi_2 - \psi_1\beta)}{\left[\psi_2 - \psi_1\beta - \frac{Pe\, k K_{AD}}{V_0}(1-\beta)\right]} \times \left[Pe\left(1 + \frac{kK_{AD}}{V_0}\right) - \frac{\Gamma}{L}(\mu_1^2 + \mu_2^2)\right]. \quad (35)$$

The parameters ψ_1 and ψ_2 contain the values of ω, Pe, and the wave numbers μ_1 and μ_2. If we consider small wavelength perturbations, this corresponds to large wave numbers, so that $-(\psi_2 - \psi_1)\, s/L \gg 1$ and therefore $\beta \approx 0$. Note that $\psi_2 < 0$. The dispersion relation can be simplified even more if we assume $-\psi_2 \gg Pek K_{AD}/V_0$, which is valid for many realistic sets of conditions. Thus:

$$\omega = \frac{PekK_{AD}}{V_0} - \frac{\Gamma}{L}(\mu_1^2 + \mu_2^2) - \chi(\mu_1^4 + \mu_2^4) \quad (36)$$

which represents ω as a polynomial function of μ_1 and μ_2. Note that the simplified dispersion relation will always lead to a principal exchange of stability.

From Eq. 36 the different phenomena can be identified as stabilizing or destabilizing effects. By noting that $\chi = D_e/V_0L^3$ and $Pe = V_0L/D_f$, we see that the rate of growth, which is related to the magnitude of the surface chemical reaction, has a destabilizing effect on the planar film. As expected surface diffusion stabilizes planar growth. These trends are consistent with what have been observed before (Mazor et al., 1988; Van den Brekel and Jansen, 1978; Ananth and Gill, 1992). It seems that gas diffusivity can have a stabilizing or destabilizing effect on planar growth. The larger the value of D_f, the smaller the first term (which is destabilizing) on the righthand side of Eq. 36, but under certain conditions V_0 increases with increasing D_f, which decreases the value of χ and thus the stabilizing effect of surface diffusion. The relative magnitude of these factors will determine the overall effect. The second term on the righthand side of Eq. 36 represents the contribution of capillarity, which tends to stabilize planar film growth.

Two-Dimensional vs. One-Dimensional Analysis

The dispersion relation is presented in Figure 2 as a function of the wave numbers μ_1 and μ_2. The dispersion relation in the plane $\mu_1 = 0$ or $\mu_2 = 0$ represents the results obtained for a one-dimensional (1-D) linear stability analysis. The critical wave number for the 1-D analysis is located in Figure 2 at the point ($\mu_1 = \mu_{cr}$, $\mu_2 = 0$, $\omega = 0$) or ($\mu_1 = 0$, $\mu_2 = \mu_{cr}$, $\omega = 0$). For the two-dimensional (2-D) analysis, this point becomes a line represented by the intersection of the dispersion relation curve with the plane $\omega = 0$. The critical wavelength, λ_{cr}, is obtained from the critical wave number by the relation $\lambda_{cr} = 2\pi/\mu_{cr}$, and it represents the minimum wavelength of perturbation which will grow with time at the specific deposition conditions. Any perturbation with a wavelength smaller than λ_{cr} will disappear with time and the basic solution is therefore stable under those conditions. One can create a plot of the critical wavelength in the y-direction as a function of that in the x-direction for the 2-D analysis. For the conditions in Table 1, such a plot is shown in Figure 3. The results reveal an interesting phenomenon. The minimum critical wavelength in the 1-D analysis is found to be higher than that in the 2-D analysis. This means that a 1-D stability analysis can predict a specific system to have a stable planar mode of deposition, while the 2-D analysis of the same system may prove that this mode is in fact unstable at those deposition conditions. It is an important result, since it means that a stability criterion identified from a simplified 1-D analysis it not necessarily valid for a system which is intrinsically two- or three-dimensional. There will be cases, however, where the stability predictions of a 1-D analysis will be more conservative than those from the 2-D analysis and in these cases the simplified analysis can be useful.

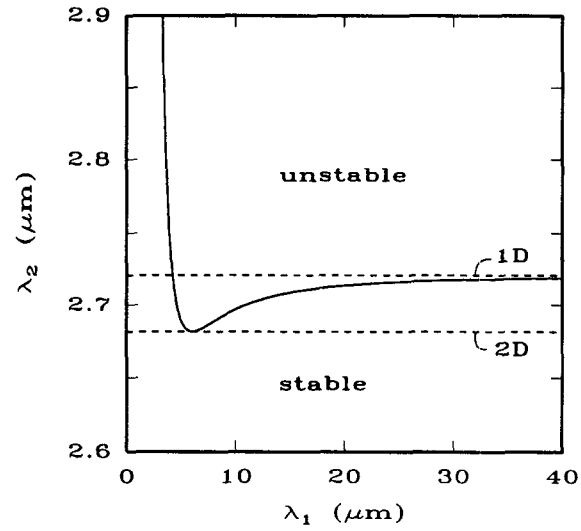

Figure 3. Neutral stability curve ($\omega = 0$), showing the difference in the minimum critical wavelength for the 1-D and 2-D stability analyses.

Effect of Reactor Conditions

In this section, we investigate the effect of reactor conditions such as temperature and reactor pressure on the linear stability criteria. This will enable one to choose reactor conditions in such a way that planar film growth can be ensured in order to produce a uniform film with the desired physical properties.

Substrate temperature

In setting up the model it is assumed that the process takes place isothermally. This enables us to study the effect of temperature on the stability of the film without having to solve an energy balance for each substrate temperature. In studying the effect of reactor conditions on the growth conditions, one has to consider different deposition modes. A typical CVD process can be limited and thus controlled by the gas diffusion through the boundary layer, the adsorption/desorption process, or the surface reaction. Physical properties and reactor conditions will be chosen to correspond to two different dep-

Table 2. Functional Form of Temperature Dependent Parameters

Parameter	Functional Form	Reference
kK_{AD}	$K_1 \exp[K_2/T]$	Froment & Bischoff (1990)
D_f	$K_3 T^{K_4}$	Bird et al. (1960)
D_e	$K_5/T \exp[K_6/T * (K_7 + K_8 T)]$	Srolovitz et al. (1988)
Γ	K_9/T	VdBrekel & Jansen (1978)

osition modes; one where deposition is reaction controlled and another where it is diffusion controlled. Specific trends can be identified by solving the dispersion relation for both sets of parameters at different temperatures. Note that the full dispersion relation is used and not the simplified equation, since the latter is subject to assumptions which may become invalid under different reactor conditions. Consider the following two cases:

(I) The deposition process is kinetically controlled, which means the chemical reaction is the limiting step. For this case, the concentration at the interface, $C_{\xi=0} \approx C_b$, over the whole range of temperature.

(II) The deposition process is essentially diffusion controlled, thus the concentration at the interface, $C_{\xi=0} \approx 0$, over the whole range of temperature.

In real CVD processes the controlling step can shift with temperature from the kinetics to diffusion, but let us focus on the two cases above. Values for the temperature independent parameters were chosen to be typical of CVD processes. The functional form of the temperature dependency of D_e, D_f, k, K_{AD}, and Γ is given in Table 2. Note that K_1 to K_9 are constants which depend on the specific system being studied. The values of the parameters chosen for the two cases are summarized in Table 3.

The adsorption equilibrium constant and the rate constant for the first-order reaction are both assumed to have an Arrhenius temperature dependence, thus $k = k_0 \exp[-E_a/R_0 T]$ and $K_{AD} = K_{AD}^0 \exp[-\Delta H_{AD}/R_0 T]$. The value of E_a is always positive, but ΔH_{AD} is usually negative, which means that adsorption/desorption and chemical reaction have opposite trends with temperature. However, the activation energy of the chemical reaction, E_a, is normally much more than the heat of adsorption, ΔH_{AD} (especially for physiosorption instead of chemisorption). For this reason we can assume that the temperature dependence of k and K_{AD} can be combined into one function where the argument of the exponent is taken as negative.

The temperature range considered is 1,000 to 1,600 K. At each temperature Eq. 25 is solved to obtain the rate of film

Table 3. Parameters Chosen to Study the Effect of Temperature on the Stability of a Planar Film

Parameter	I: Reaction-Controlled	II: Diffusion-Controlled
s (m)	10^{-3}	10^{-3}
δ (m)	10^{-10}	10^{-10}
ρ	10^{-5}	10^{-5}
kK_{AD} (m/s)	$10^2 \exp[-11{,}052/T]$	$10^4 \exp[-11{,}052/T]$
D_f (m^2/s)	$5 \times 10^{-8} T^{1.823}$	$5 \times 10^{-13} T^{1.823}$
D_e (m^4/s)	•	•
Γ (m)	$8 \times 10^{-9}/T$	$8 \times 10^{-9}/T$

• $\equiv [(1.687 \times 10^{-19})/T] \exp[-2{,}000/T(5.0 + 0.0033T)]$.

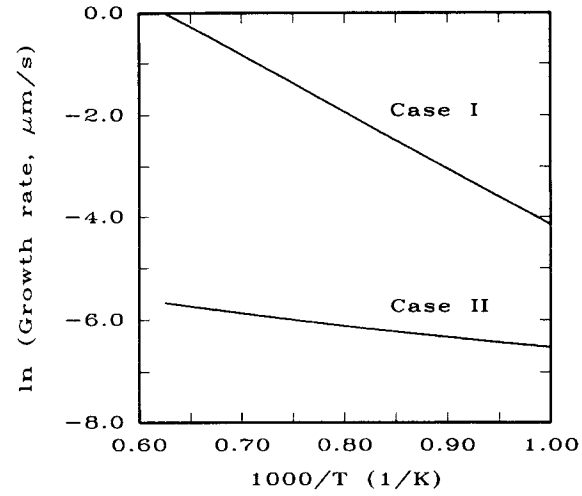

Figure 4. Effect of temperature of deposition rate when chemical reaction controls (case I), and when gas diffusion controls (case II) the process.

growth V_0 under planar deposition conditions. This value is then used in the dispersion relation (Eq. 34) at neutral stability ($\omega = 0$) to determine the critical wave number in the η-direction as a function of the critical wave number in the ξ-direction. The critical wavelength is obtained from its inverse relation to the wave number.

The effect of temperature on the deposition rate is shown in Figure 4. In both cases the deposition rate increases with temperature. However, the functional form of the increase is different. When the chemical reaction controls (case *I*), the slope of the curve and thus the apparent activation energy of the process is much larger than in the case of diffusion-controlled deposition (case *II*). Under reaction-controlled conditions, the Arrhenius temperature dependence of the rate constant dominates other temperature dependencies, while the effect of gas diffusion is more important in case *II*. This results in a much more gradual increase in deposition rate under those conditions. The increase in the growth rate with temperature is consistent with what is expected in a CVD process and with what has been observed experimentally (Chin et al., 1977; Paretta et al., 1991).

The effect of temperature on the linear stability of the flat surface is shown in Figures 5a and 5b. At each temperature the neutral stability curve is drawn in the form of the critical wavelength in the η-direction as a function of the critical wavelength in the ξ-direction. The curve separates the unstable and stable regions. If the wavelengths of perturbation correspond to a point above and to the right of the curve, that perturbation will grow in time and the flat interface is unstable.

To the left and below the curve is the stable region. Note that when the deposition is reaction controlled (Figure 5a), the minimum critical wavelength decreases with temperature, which means the unstable region becomes larger with temperature. A perturbation with wavelengths λ_1, $\lambda_2 = 30$ μm is in the stable region at a temperature of 1,000 K, but in the unstable region at 1,600 K. There seems to be some agreement between this trend and the observation in many CVD processes that the surface morphology becomes less smooth as the substrate temperature is increased (Chin et al., 1977; Hartmann et al., 1991).

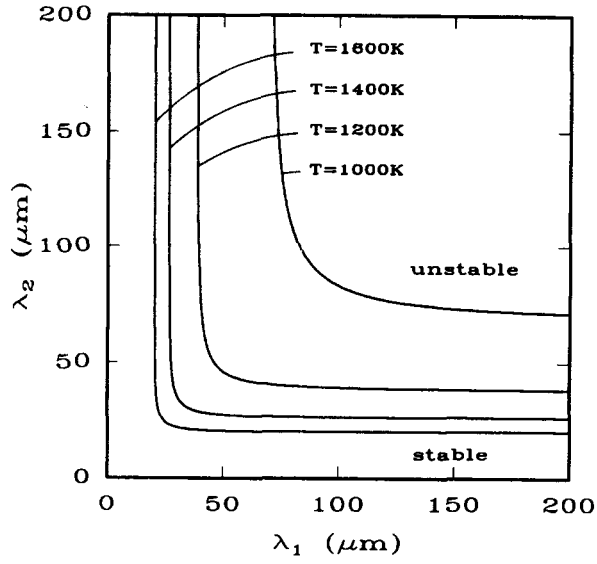

Figure 5a. Effect of temperature on linear stability when chemical reaction controls.

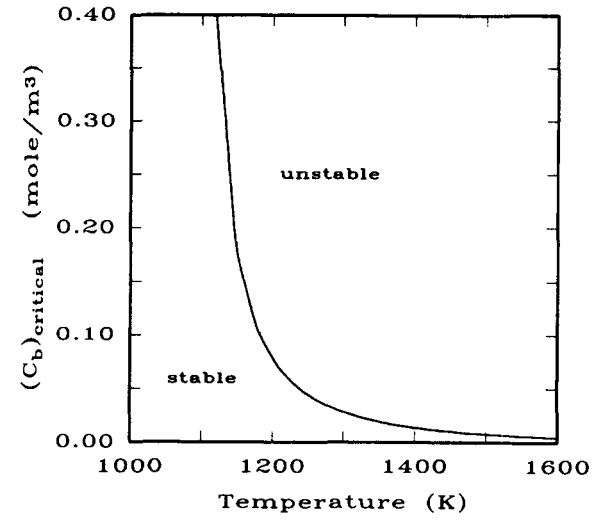

Figure 6a. Effect of temperature on the critical bulk concentration when chemical reaction controls (for λ_1, $\lambda_2 = 50$ μm).

Note, however, that a linear stability analysis cannot predict the form of the nonlinear solution when the planar solution becomes unstable. Under those conditions the model equations have to be solved numerically.

When gas diffusion controls the deposition process, the model predicts an increase in the minimum critical wavelength with temperature, which means the flat surface becomes more stable at higher substrate temperatures. The reason is that adatom mobility increases with temperature which results in a stronger surface diffusion effect. This stabilizes planar film growth.

An alternative method of controlling the deposition morphology of the solid film is to keep the substrate temperature fixed and to adjust the gas concentration in the bulk phase. If one chooses specific wavelengths of perturbation in the x and y directions for a fixed temperature, one can determine the maximum bulk concentration at which planar growth will still be stable. Figure 6 presents the results for the two cases defined by the parameters in Table 3, thus for a reaction controlled (Figure 6a) and a diffusion controlled (Figure 6b) CVD process. The wavelengths of perturbation in Figure 6a are λ_1, $\lambda_2 = 50$ μm, and those in Figure 6b are λ_1, $\lambda_2 = 2$ μm. Once again there is a different trend for the reaction and diffusion controlled processes. If the temperature is increased in the reaction controlled process, the maximum bulk concentration decreases, whereas it increases for the diffusion controlled process.

Reactor pressure

The reactor pressure is an important parameter in the operation of vapor deposition processes. Physical vapor deposition processes are carried out under high vacuum where the deposition mechanism is ballistic. In CVD processes, the re-

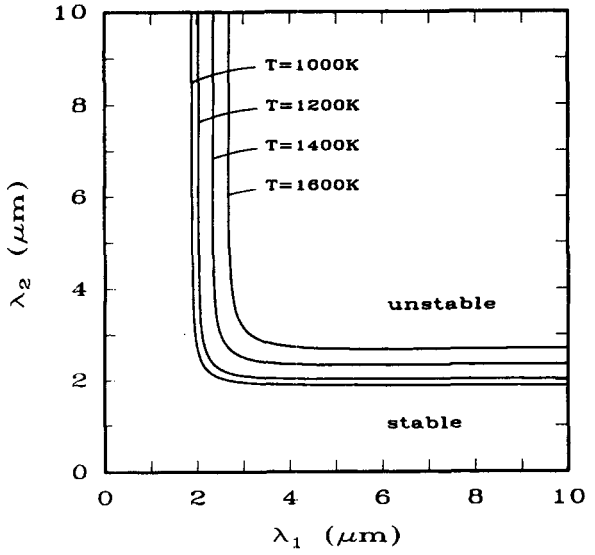

Figure 5b. Effect of temperature on linear stability when gas diffusion controls the process.

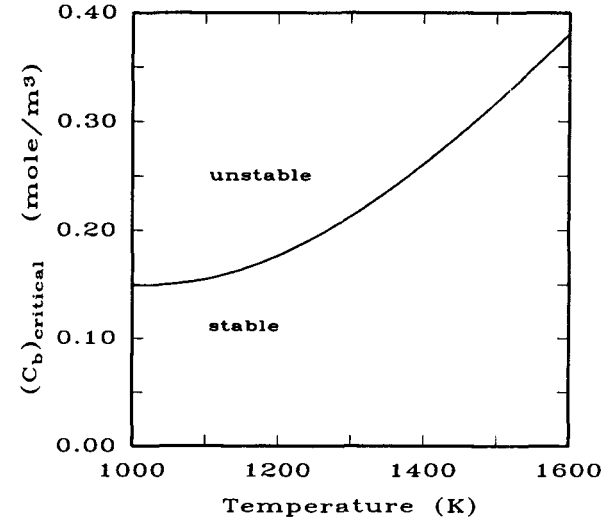

Figure 6b. Effect of temperature on the critical bulk concentration when gas diffusion controls the process (for λ_1, $\lambda_2 = 2$ μm).

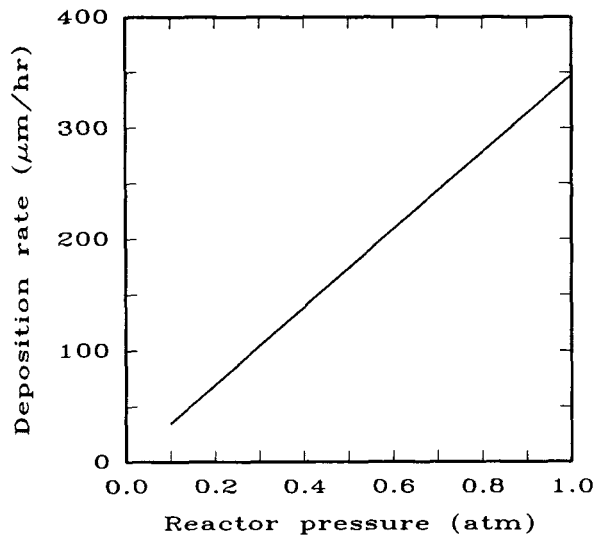

Figure 7. Effect of reactor pressure on the deposition rate when chemical reaction controls the process.

actor pressure is usually much higher, typically 10^{-3} to 1 atm. The gas diffusivity is enhanced by a decrease in pressure, so low pressure operation is preferred. Usually, under low pressure conditions, the chemical reaction is rate controlling, rather than the mass-transfer processes. We will consider a case where the substrate temperature is fixed and study the effect of reactor pressure on the stability of the planar film.

In a typical CVD process, the reactants are fed in very dilute concentrations in the gas phase, with 90 to 99% dilution. The reactant concentration increases in proportion to the reactor pressure if a constant dilution ratio is maintained. This enhances the surface reaction, which leads to enhanced film growth. However, gas diffusivity is inversely proportional to reactor pressure at constant temperature and low to moderate pressures ($D_f \propto 1/P$), which results in a lower concentration of reactant on the surface. These two effects oppose each other

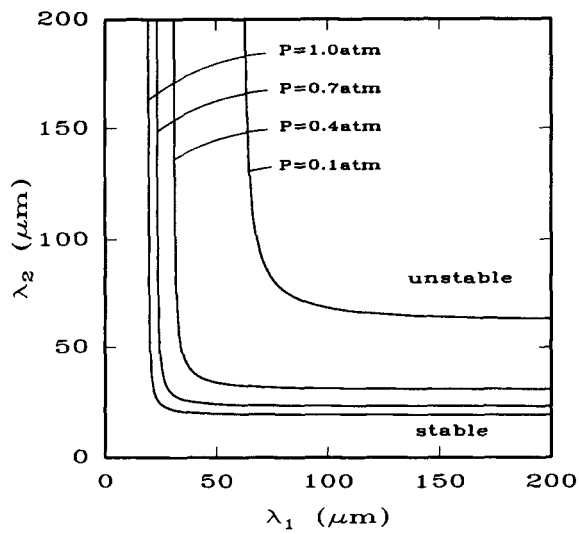

Figure 8. Effect of reactor pressure on linear stability when chemical reaction controls the process.

and a balance (which depends on the specific system) exists between them.

By using a fixed substrate temperature of 1,400 K and a constant dilution ratio of 95%, we determined the deposition rate and the critical wavelengths at increasing pressures. The parameters of case I in the previous section were used (at $T = 1{,}400$ K), thus a process which is kinetically controlled.

The results are shown in Figures 7 and 8. The deposition rate increases linearly with increasing pressure, due to the linear increase in the bulk concentration of reactants. It seems that the decrease in the gas diffusivity with pressure has virtually no inhibiting effect on the deposition rate for the chosen set of parameters.

The effect of reactor pressure on the stability of the planar film solution is shown in Figure 8. Four different pressures were chosen, as well as the neutral stability curves presented in the form of the critical wavelength in the η-direction as a function of that in the ξ-direction. The region above and to the right of a curve represents the unstable region. The results indicate that the minimum critical wavelength decreases with increasing pressure. This means that a solid film which is growing in the stable planar mode at a certain reactor pressure, can become unstable if the pressure is increased. This is consistent with predicted trends (Ananth and Gill, 1992).

Summary and Conclusions

The tremendous growth of the computer industry has placed increasingly stringent demands on the thin film products of the microelectronics industry. It has become necessary to control the purity, composition, thickness, microstructure, and surface morphology of these films extremely accurately. This article deals with a very important aspect of film deposition, the morphology. Experimental observations of film morphology in vapor deposition processes have in some cases been contradictory to expectations. We focused on solid films produced by CVD and attempted to confirm the trends observed experimentally.

An isothermal two-dimensional model was developed which describes the growth of a solid-gas interface during a typical CVD process. The effects of gas diffusion through the boundary layer, adsorption/desorption, a surface chemical reaction, surface diffusion, capillarity, and the local curvature of the film were included in the model. The model equations represent a system of coupled nonlinear partial differential equations which cannot be solved analytically. However, a linear stability analysis of the planar solution yields valuable information about the deposition conditions. It was found that the surface chemical reaction has a destabilizing effect on planar film growth, while surface diffusion and capillarity was found to stabilize planar film growth. It was found that the gas diffusivity can stabilize or destabilize planar growth depending on the system conditions.

The results were compared with those obtained when one horizontal coordinate direction is neglected. It was found that for some conditions the simpler 1-D analysis predicted different critical conditions than the 2-D analysis. This illustrates that the stability criteria found for a system in 1-D is not necessarily valid if the real system has more than one dimension.

The effect of reactor conditions on the stability of the planar solution was studied. It was found that an increase in the

substrate temperature resulted in an increase in the deposition rate, mainly due to an increased rate of chemical reaction. This is consistent with experimental observations. The effect of temperature on the stability of the flat interface depends on which phenomenon controls the deposition process. If the process is reaction controlled, the stability of the flat interface is adversely affected by high temperature. This is consistent with the trend that has generally been observed experimentally. However, in the diffusion-limited regime, an increase in temperature seems to improve the stability of the planar mode.

Most CVD processes are carried out at low pressure ($0.01 \le P < 1.0$ atm), since the gas diffusivity increases with decreasing pressure. The model predicts that an increase in reactor pressure enhances the deposition rate, but decreases the stability of the planar surface. This trend is consistent with previous results.

Notation

a = constant, given by $[(V_0+kK_{AD})/kK_{AD}]/\{(V_0+kK_{AD})/kK_{AD}-\exp[-Pes/L]\}$
A = constant in Eq. 31
b = constant, given by $-1/\{V_0+kK_{AD})/kK_{AD}-\exp[-Pes/L]\}$
B = constant in Eq. 31
C = gas concentration, mol/m^3
C_b = concentration of reactant in bulk flow, mol/m^3
C_s = concentration of reactant adsorbed on the surface, mol/m^2
C^* = function of ζ, defined in Eq. 28
$\mathcal{C}$ = dimensionless concentration, subscripts: 0 = basic; 1 = perturbed
D_e = effective surface diffusion coefficient, m^4/s
D_f = gas diffusion coefficient, m^2/s
D_s = surface diffusion coefficient, m^2/s
E_a = activation energy, J/mol
h = height of film, m
H = dimensionless height of film
H^* = constant, defined in Eq. 29
ΔH_{AD} = heat of adsorption, J/mol
J = flux of reactant, m/s
k = reaction rate constant, 1/s
Kn = Knudsen number, MFP/distance between source and substrate
K_0 = preexponential factor, 1/s
$\mathcal{K}_1$ = surface curvature, $-h_{xx}/[(1+h_x^2+h_y^2)^{3/2}]$, m^{-1}
$\mathcal{K}_2$ = surface curvature, $-h_{yy}/[(1+h_x^2+h_y^2)^{3/2}]$, m^{-1}
K_{AD} = adsorption/desorption equilibrium constant, m
K_{AD}^0 = preexponential factor, m
K_BT = thermal energy, J
L = characteristic length scale, $\sqrt{D_e/\delta V_0}$, m
n = vector normal to surface
Pe = Peclet number, V_0L/D_f
$R(C)$ = reaction term, mol/m^2·s
R_0 = universal gas constant, J/mol·K
s = boundary layer thickness, m
Δs = element of surface, m^2
SZM = structure zone models
t = time, s
T = substrate temperature, K
T_m = melting point of coating material, K
T_s = surface temperature, K
V_0 = growth speed, or deposition rate, m/s
x = horizontal coordinate, m
y = horizontal coordinate, m
z = vertical coordinate, m

Greek symbols

α = number of molecules per unit surface area, 1/m^2
β = $\exp[(\psi_2-\psi_1)s/L]$
γ = molar volume, m^3/mol
Γ = Capillary length, m
δ = radius of molecule, m
ϵ = perturbation parameter
ζ = vertical coordinate, dimensionless
η = horizontal coordinate, dimensionless
κ_1 = dimensionless surface curvature, $-H_{\xi\xi}/[(1+H_\xi^2+H_\eta^2)^{3/2}]$
κ_2 = dimensionless surface curvature, $-H_{\eta\eta}/[(1+H_\xi^2+H_\eta^2)^{3/2}]$
λ = wavelength of perturbation, $2\pi/\mu$
μ = wave number of perturbation
ξ = horizontal coordinate, dimensionless
ρ = dimensionless parameter, equivalent to γC_b
σ_s = surface energy density, N/m
τ = dimensionless time, tV_0/L
Υ = surface tension, N/m
χ = dimensionless parameter, equivalent to D_e/V_3L^3
$\psi_{1,2}$ = defined by Eq. 32
ω = eigenvalue
Ω = volume of molecule, m^3

Subscripts

cr = at critical conditions
I = imaginary part
R = real part
1 = in x or ξ direction
2 = in y or η direction
3 = in z or ζ direction

Literature Cited

Ananth, R., and W. N. Gill, "Criteria for Making Uniform Films by Chemical Vapor Deposition," *J. Crystal Growth*, **118**, 60 (1992).
Bales, G. S., A. C. Redfield, and A. Zangwill, "Growth Dynamics of Chemical Vapor Deposition," *Phys. Rev. Lett.*, **62**(7), 776 (1989).
Bales, G. S., and A. Zangwill, "Macroscopic Model for Columnar Growth of Amorphous Films by Sputter Deposition," *J. Vac. Sci. Technol. A*, **9**(1), 145 (1991).
Bernoff, A. J., and S. Lichter, "Continuum Model of Thin-Film Deposition and Growth," *Phys. Rev. B*, **39**(15), 10560 (1989).
Bird, R. B., W. E. Stewart, and E. N. Lightfoot, *Transport Phenomena*, John Wiley, New York (1960).
Blech, I. A., "Evaporated Film Profiles Over Steps in Substrates," *Thin Solid Films*, **6**, 113 (1970).
Bunshah, R. F., ed., *Deposition Technologies for Films and Coatings*, Noyes Publications, Park Ridge, NJ (1982).
Chin, J., P. K. Gantzel, and R. G. Hudson, "The Structure of Chemical Vapor Deposited Silicon Carbide," *Thin Solid Films*, **40**, 57 (1977).
Cooke, M. J., and G. Harris, "Monte Carlo Simulation of Thin Film Deposition in a Rectangular Groove," *J. Vac. Sci. Technol. A*, **7**(6), 3217 (1989).
Dirks, A. G., and H. J. Leamy, "Columnar Microstructure in Vapor-Deposited Thin Films," *Thin Solid Films*, **47**, 219 (1977).
Friedlander, S. K., *Smoke, Dust and Haze*, Wiley, New York (1977).
Froment, G. F., and K. B. Bischoff, *Chemical Reactor Analysis and Design*, 2nd ed., John Wiley, New York (1990).
Habig, K.-H., "CVD and PVD Coatings: Properties, Tribological Behavior, and Applications," *J. Vac. Sci. Technol. A*, **4**(6), 2832 (1986).
Hartmann, H., L. Hildisch, E. Krause, and W. Mohling, "Morphological Stability and Crystal Structure of CVD-Grown Zinc Selenide," *J. Mater. Sci.*, **26**, 4917 (1991).
Henderson, D., M. H. Brodsky, and P. Chaudhari, "Simulation of Structural Anisotropy and Void Formation in Amorphous Thin Films," *Appl. Phys. Lett.*, **25**(11), 641 (1974).
Kardar, M., G. Parisi, and Y.-C. Zhang, "Dynamic Scaling of Growing Interfaces," *Phys. Rev. Lett.*, **56**(9), 889 (1986).
Koo, K.-K., R. Ananth, and W. N. Gill, "Thermal Convection, Morphological Stability and the Dendritic Growth of Crystals," *AIChE J.*, **38**(6), 945 (1992).
Lichter, S., and J. Chen, "Model for Columnar Microstructure of Thin Solid Films," *Phys. Rev. Lett.*, **56**(13), 1396 (1986).
Mazor, A., B. G. Bukiet, and D. J. Srolovitz, "The Effect of Vapor

Incidence Angle Upon Thin-Film Columnar Growth," *J. Vac. Sci. Technol. A*, 7(3), 1386 (1989).
Mazor, A., D. J. Srolovitz, P. S. Hagen, and B. G. Bukiet, "Columnar Growth in Thin Films," *Phys. Rev. Lett.*, **60**(5), 424 (1988).
Messier, R., "Toward Quantification of Thin Film Morphology," *J. Vac. Sci. Technol. A*, **4**(3), 490 (1986).
Messier, R., and J. E. Yehoda, "Geometry of Thin-Film Morphology," *J. Appl. Phys.*, **58**(10), 3739 (1985).
Movchan, B. A., and A. V. Demchishin, "Study of the Structure and Properties of Thick Vacuum Condensates of Nickel, Titanium, Tungsten, Aluminum Oxide and Zirconium Dioxide," *Fiz. Metal. Metalloved.*, **28**(4), 653 (1969).
Mullins, W. W., "Theory of Thermal Grooving," *J. Appl. Phys.*, **28**(3), 333 (1957).
Mullins, W. W., and R. F. Sekerka, "Stability of a Planar Interface During Solidification of a Dilute Binary Alloy," *J. Appl. Phys.*, **35**(2), 444 (1964).
Palmer, B. J., and R. G. Gordon, "Local Equilibrium Model of Morphological Instabilities in Chemical Vapor Deposition," *Thin Solid Films*, **158**, 313 (1988).
Palmer, B. J., and R. G. Gordon, "Kinetic Model of Morphological Instabilities in Chemical Vapor Deposition," *Thin Solid Films*, **177**, 141 (1989).
Paretta, A., A. Camanzi, G. Giunta, and A. Mazzarano, "Morphological Aspects of Silicon Carbide Chemically Vapour-Deposited on Graphite," *J. Mater. Sci.*, **26**, 6057 (1991).
Pelce, P., ed., *Dynamics of Curved Fronts*, Academic Press, Boston, MA (1988).
Raguram, A. C., and R. F. Bunshah, "The Effect of Substrate Temperature on the Structure of Titanium Carbide Deposited by Activated Reactive Evaporation," *J. Vac. Sci. Technol.*, **9**(6), 1389 (1972).
Roenigk, K. F., and K. F. Jensen, "Analysis of Multicomponent LPCVD Processes," *J. Electrochem. Soc.*, **132**(2), 448 (1985).
Schmidt, W. U., "The Development of Chromium Diboride Fibers by CVD for Use as Reinforcement Material in Metal Matrix Composites," MS Thesis, SUNY at Buffalo, NY (1991).
Srolovitz, D. J., "Grain Growth Phenomena in Films: A Monte Carlo Approach," *J. Vac. Sci. Technol. A*, **4**(6), 2925 (1986).
Srolovitz, D. J., A. Mazor, and B. G. Bukiet, "Analytical and Numerical Modeling of Columnar Evolution in Thin Films," *J. Vac. Sci. Technol. A*, **6**(4), 2371 (1988).
Tait, R. N., T. Smy, and M. J. Brett, "Simulation and Measurement of Density Variation in Mo Films Sputter Deposited Over Oxide Steps," *J. Vac. Sci. Technol. A*, **8**(3), 1593 (1990).
Thornton, J. A., "Influence of Apparatus Geometry and Deposition Conditions on the Structure and Topography of Thick Sputtered Coatings," *J. Vac. Sci. Technol.*, **11**(4), 666 (1974).
Van den Brekel, C. H. J., and A. K. Jansen, "Morphological Stability Analysis in Chemical Vapour Deposition Processes I," *J. Crystal Growth*, **43**, 364 (1978).
Van den Brekel, C. H. J., and A. K. Jansen, "Morphological Stability Analysis in Chemical Vapour Deposition Processes II," *J. Crystal Growth*, **43**, 371 (1978).
Vossen, J. L., and W. Kern, eds., *Thin Film Processes*, Academic Press, New York (1978).
Vossen, J. L., and W. Kern, eds., *Thin Film Processes II*, Academic Press, New York (1991).

Appendix I

Derivation of the equation for surface evolution

The position of the interface at time t in the two-dimensional space is given by $h(x, y, t)$. Consider a small element of the surface as indicated in Figure A1. Δs_0 is the element of the actual surface of the evolving film which is at a height $h(x_0, y_0, t)$. The center of a molecule or a cluster of molecules (with monolayer thickness) on the surface is at a distance δ above the surface. This means that it can be assumed the deposition does not take place on the actual surface, but on an imaginary surface which is displaced by a distance δ from the actual surface. The corresponding size of a surface element is then either larger or smaller than the actual surface, depending on the curvature $\mathcal{K}$. This means that an element of the surface receives a number of molecules greater (for $\mathcal{K}>0$) or smaller (for $\mathcal{K}<0$) than the flux to a flat surface. (However, it also takes a greater number (for $\mathcal{K}>0$) or fewer (for $\mathcal{K}<0$) molecules to build up a film of the same thickness.)

The concern of the projection on the xy-plane of surface element Δs_0 are given by the points x_0, $x_0+\Delta x$, y_0, and $y_0+\Delta y$. We use the fact that a unit vector normal to $h(x_0, y_0, t)$ is given by:

$$n=\left[-\frac{h_x(x_0, y_0, t)}{\sqrt{1+h_x^2(x_0, y_0, t)+h_y^2(x_0, y_0, t)}},\right.$$
$$-\frac{h_y(x_0, y_0, t)}{\sqrt{1+h_x^2(x_0, y_0, t)+h_y^2(x_0, y_0, t)}},$$
$$\left.\frac{1}{\sqrt{1+h_x^2(x_0, y_0, t)+h_y^2(x_0, y_0, t)}}\right]. \quad \text{(A1)}$$

The corners of the projection on the xy-plane of the corresponding imaginary surface element are given by the points:

$$x_L=x_0-\frac{\delta h_x(x_0, y_0, t)}{\sqrt{1+h_x^2(x_0, y_0, t)+h_y^2(x_0, y_0, t)}},$$
$$y_L=y_0-\frac{\delta h_y(x_0, y_0, t)}{\sqrt{1+h_x^2(x_0, y_0, t)+h_y^2(x_0, y_0, t)}},$$
$$x_R=x_0+\Delta x-\frac{\delta h_z(x_0+\Delta x, y_0, t)}{\sqrt{1+h_x^2(x_0+\Delta x, y_0, t)+h_y^2(x_0+\Delta x, y_0, t)}},$$
$$y_R=y_0+\Delta y-\frac{\delta h_y(x_0, y_0+\Delta y, t)}{\sqrt{1+h_x^2(x_0, y_0+\Delta y, t)+h_y^2(x_0, y_0+\Delta y, t)}}. \quad \text{(A2)}$$

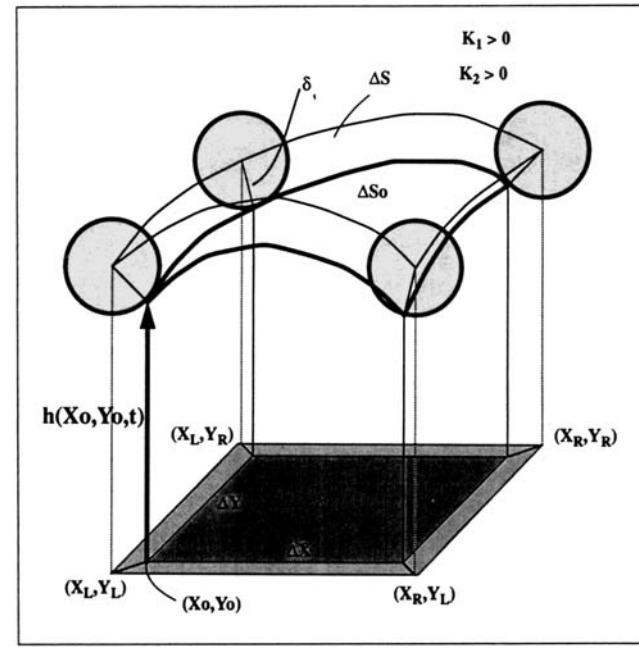

Figure A1. Surface element of curved interface.

An element of the actual surface is given by:

$$\Delta s_0 = \int_{y_0}^{y_0+\Delta y}\int_{x_0}^{x_0+\Delta x} \sqrt{1+h_\xi^2(\xi,\eta,t)+h_\eta^2(\xi,\eta,t)}\,d\xi\,d\eta \approx \sqrt{1+h_x^2(x_0,y_0,t)+h_y^2(x_0,y_0,t)}\,\Delta x\,\Delta y. \quad \text{(A3)}$$

The imaginary surface element is thus given by:

$$\Delta s = \int_{y_L}^{y_R}\int_{x_L}^{x_R} \sqrt{1+h_\xi^2(\xi,\eta,t)+h_\eta^2(\xi,\eta,t)}\,d\xi\,d\eta.$$

Thus,

$$\Delta s \approx \sqrt{1+h_x^2+h_y^2}\,[\Delta x-(\square)][\Delta y-(\diamond)] \quad \text{(A4)}$$

where

$$\square = \frac{\delta h_x(x_0+\Delta x, y_0+\Delta y, t)}{\sqrt{1+h_x^2(x_0+\Delta x, y_0+\Delta y, t)+h_y^2(x_0+\Delta x, y_0+\Delta y, t)}} - \frac{\delta h_x(x_0,y_0,t)}{\sqrt{1+h_x^2(x_0,y_0,t)+h_y^2(x_0,y_0,t)}},$$

$$\diamond = \frac{\delta h_y(x_0+\Delta x, y_0+\Delta y, t)}{\sqrt{1+h_x^2(x_0+\Delta x, y_0+\Delta y, t)+h_y^2(x_0+\Delta x, y_0+\Delta y, t)}} - \frac{\delta h_y(x_0,y_0,t)}{\sqrt{1+h_x^2(x_0,y_0,t)+h_y^2(x_0,y_0,t)}}.$$

In simplified form:

$$\Delta s = \sqrt{1+h_x^2+h_y^2}\,\Delta x\,\Delta y \times\left(1-\left[\frac{\delta h_x}{\sqrt{1+h_x^2+h_y^2}}\right]_x\right)\left(1-\left[\frac{\delta h_y}{\sqrt{1+h_x^2+h_y^2}}\right]_y\right). \quad \text{(A5)}$$

Conservation of mass in the time period t and $t+\Delta t$ requires the following equation to hold:

$$[\bar{h}(t+\Delta t)-\bar{h}(t)](x_R-x_L)(y_R-y_L)=\gamma D_f(\nabla C\cdot n)\Delta t\Delta s$$

where $h(t)$ indicates the average of h in the x and y directions within the element $(x_R-x_L)(y_R-y_L)$ at time t. Thus, the left-hand side of the conservation equation is given by:

$$[\bar{h}(t+\Delta t)-\bar{h}(t)]\Delta x\Delta y \times\left(1-\left[\frac{\delta h_x}{\sqrt{1+h_x^2+h_y^2}}\right]_x\right)\left(1-\left[\frac{\delta h_y}{\sqrt{1+h_x^2+h_y^2}}\right]_y\right) \quad \text{(A6)}$$

and the righthand side by:

$$\gamma D_f(\nabla C\cdot n)\Delta t\sqrt{1+h_x^2+h_y^2}\,\Delta x\Delta y \times\left(1-\left[\frac{\delta h_x}{\sqrt{1+h_x^2+h_y^2}}\right]_x\right)\left(1-\left[\frac{\delta h_y}{\sqrt{1+h_x^2+h_y^2}}\right]_y\right). \quad \text{(A7)}$$

Divide by $\Delta x\Delta y\Delta t$ and take the limit where Δx, Δy, $\Delta t\to 0$:

$$h_t=\gamma D_f(\nabla C\cdot n)\sqrt{1+h_x^2+h_y^2}. \quad \text{(A8)}$$

Note that:

$$\nabla C\cdot n = -\frac{\partial C}{\partial x}\frac{h_x}{\sqrt{1+h_x^2+h_y^2}} - \frac{\partial C}{\partial y}\frac{h_y}{\sqrt{1+h_x^2+h_y^2}} + \frac{\partial C}{\partial z}\frac{1}{\sqrt{1+h_x^2+h_y^2}} \quad \text{(A9)}$$

thus:

$$h_t=h_xJ_1+h_yJ_2+J_3 \quad \text{(A10)}$$

where J_1, J_2, and J_3 are the flux components (at $z=h$) in the x, y, and z directions, respectively:

$$J_1=-\gamma D_f\frac{\partial C}{\partial x},$$

$$J_2=-\gamma D_f\frac{\partial C}{\partial y},$$

$$J_3=\gamma D_f\frac{\partial C}{\partial z}.$$

The surface diffusion also plays an important role in the evolution of the film. The contribution of surface diffusion to the surface evolution is given by (Mullins, 1957; Srolovitz et al., 1988):

$$h_t=-D_e\left[\left(\frac{1}{\sqrt{1+h_x^2+h_y^2}}\left[\frac{h_{xx}}{(1+h_x^2+h_y^2)^{3/2}}\right]_x\right)_x + \left(\frac{1}{\sqrt{1+h_x^2+h_y^2}}\left[\frac{h_{yy}}{(1+h_x^2+h_y^2)^{3/2}}\right]_y\right)_y\right]. \quad \text{(A11)}$$

Combining the two contributions to the surface evolution, one finds:

$$h_t=h_xJ_1+h_yJ_2+J_3 + D_e\left(\left[\frac{\mathcal{K}_{1x}}{\sqrt{1+h_x^2+h_y^2}}\right]_x+\left[\frac{\mathcal{K}_{2y}}{\sqrt{1+h_x^2+h_y^2}}\right]_y\right) \quad \text{(A12)}$$

where $\mathcal{K}_1$ and $\mathcal{K}_2$ are the curvatures in the x and y directions, respectively:

$$\mathcal{K}_1=-\frac{h_{xx}}{(1+h_x^2+h_y^2)^{3/2}},\quad \mathcal{K}_2=-\frac{h_{yy}}{(1+h_x^2+h_y^2)^{3/2}}. \quad \text{(A13)}$$

Manuscript received Nov. 30, 1992, and revision received Sept. 16, 1993.